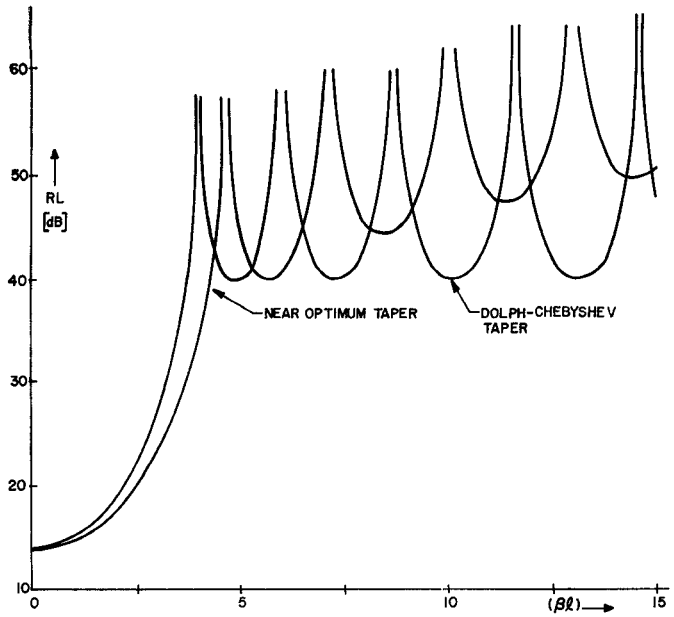

Fig. 6. Return loss versus (βl) of 50–75-Ω matching sections.

$\epsilon_{max} \cong 0.0493$. Using Table I, we first obtain by linear interpolation

$$B = 3.3727 \quad \text{and} \quad (\beta l)_{min} = 4.2302.$$

$(\beta l)_{min}$ determines the minimum length for given lowest frequency, whereas B determines with $G(B, \xi)$ the impedance variation. Table II shows values of the characteristic impedance Z_c along the x coordinate of the near-optimum taper as computed with the aid of Table I and by linear interpolation. The error made due to the interpolation is less than 0.2 percent.

Fig. 5 depicts the impedance variation along the axis of the transmission line for the optimum and near-optimum taper. It is worthwhile to note that the near-optimum taper needs a minimum length of 0.6733 λ, whereas the value for the optimum taper is 0.5871 λ. This is an increase by only less than 13 percent. In Fig. 6, the return loss for the near-optimum matching section has been plotted to be compared with the performance of the optimum Dolph–Chebyshev Taper.

References

[1] R. W. Klopfenstein, "A transmission line taper of improved design," *Proc. IRE*, vol. 44, pp. 31–35, Jan. 1956.
[2] L. Solymar, "Spurious mode generation in nonuniform waveguide," *IRE Trans. Microwave Theory Tech.*, vol. MTT-7, pp. 379–383, July 1959.
[3] R. E. Collin, "The optimum tapered transmission line matching section," *Proc. IRE*, vol. 44, pp. 539–548, Apr. 1956.
[4] L. R. Walker and N. Wax, "Nonuniform transmission-lines and reflection coefficients," *J. Appl. Phys.*, vol. 17, pp. 1043–1045, 1945.
[5] R. E. Collin, *Foundations for Microwave Engineering*. New York: McGraw-Hill, 1966.
[6] I. M. Ryshik and I. S. Gradstein, *Tables of Series, Products and Integrals*. Berlin, Germany: Verlag der Deutschen Wissenschaften, 1963.
[7] C. R. Burrus, "The exponential transmission-line," *Bell. Syst. Tech. J.*, vol. 17, pp. 555–573, 1938.
[8] R. C. Hansen, *Microwave Scanning Antennas*, vol. I. New York: Academic Press, 1964.

Propagation Characteristics of a Rectangular Waveguide Containing a Cylindrical Rod of Magnetized Ferrite

TOSHIO YOSHIDA, MASAYOSHI UMENO, AND SHICHIRO MIKI

Abstract—**With an axially magnetized cylindrical ferrite rod inserted into a rectangular waveguide parallel to the *E*-field of the dominant (TE_{10}) mode, the electromagnetic field amplitudes inside the ferrite rod and the transmission and reflection coefficients are numerically obtained by means of a digital computer and their results are shown in figures. At resonance, the distributions of RF magnetization and electric field have good symmetrical patterns in the cross section of the rod.**

The experimental results of the transmission and reflection coefficients agree well with the theoretical values.

Manuscript received December 29, 1971; revised May 30, 1972. Part of this work was presented at the International Symposium on Antennas and Propagation, Japan, September 1971.

The authors are with the Department of Electronic Engineering, Nagoya University, Nagoya, Japan.

I. Introduction

THE RESONANCE phenomena of ferrite samples have been investigated by a number of authors. Among these investigations, the problems concerning propagation characteristics and field distributions in the waveguide containing a ferrite sample are of interest in view of both experiments and theories, because they are important to the studies of the nonreciprocal devices and the conversion from electromagnetic waves to magnetic waves [1]. However, the field distribution inside the ferrite sample and the detailed transmission and reflection coefficients have not been reported.

Much fundamental information on these problems is obtained by studying the case of the waveguide containing a circular cylindrical ferrite rod inserted parallel to the E-field of the dominant mode in a rectangular waveguide and axially magnetized by an external static magnetic field.

An analysis of this situation was discussed first by Epstein and Berk [2]. They successively introduced the scattered wave from the rod and the mirrored waves from the guide walls to satisfy the boundary conditions. However, it would not only be difficult but unfeasible to obtain an approximate solution of higher order than the first, because of its cumbersome nature. But in order to obtain more precisely the field distributions inside the rod and the transmission and reflection coefficients, we need the higher order approximate or rigorous solution. Okamoto *et al.* obtained the rigorous solution of this problem by taking account of an infinite number of images of the rod with respect to the guide walls [3]. However, they did not give any results of numerical computation about the field distributions.

In this paper the numerical results for the transmission and reflection coefficients and the amplitude of the field inside the rod [4] are shown. We illustrate clearly in figures two types of resonance phenomena: the magnetostatic mode and the standing wave mode.

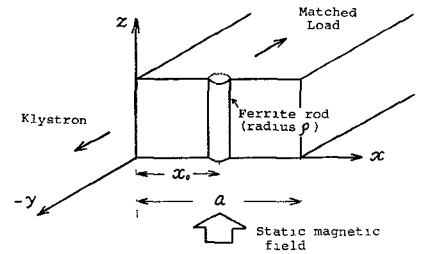

Fig. 1. Rectangular waveguide inserted with a cylindrical ferrite rod.

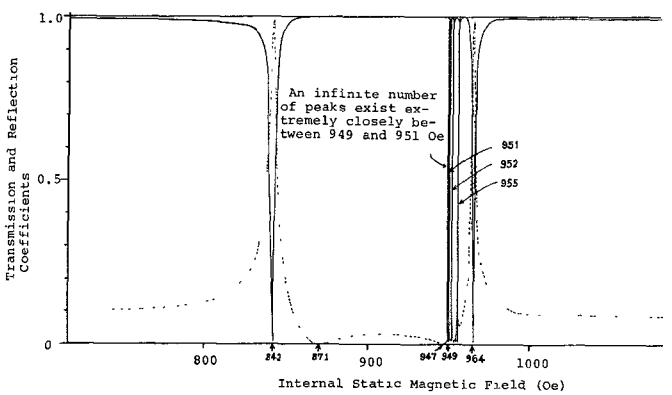

Fig. 2. Amplitudes of transmission coefficient (solid line) and reflection coefficient (dotted line) as a function of internal static magnetic field intensity.

II. Computed Results

The general theory has been formulated in [3], and therefore it is not repeated here. However, in practical computations it is necessary to note that in the notation of [3, eq. (17)],

$$\sin^{-1} t = \pi - (\sin^{-1} t)_p, \quad \{f_t = 1 \cdots |t| \le 1 \quad (1)$$

$$\sqrt{1-t^2} = f_t \cdot (\sqrt{1-t^2})_p, \quad \{f_t = -1 \cdots |t| > 1 \quad (2)$$

where $(\sin^{-1} t)_p$ and $(\sqrt{1-t^2})_p$ denote the principal roots of $\sin^{-1} t$ and $\sqrt{1-t^2}$, respectively.

In this section, the results are shown for both the transmission and reflection coefficients and the EM field distributions, which are computed by means of a digital computer.

In the lossy ferrite sample, μ and κ in [3, eq. (4)] are expressed by

$$\mu = 1 + \frac{(\omega_H + j/\tau_{rel})\omega_M}{(\omega_H + j/\tau_{rel})^2 - \omega^2}$$

$$\kappa = \frac{\omega\omega_M}{(\omega_H + j/\tau_{rel})^2 - \omega^2} \quad (3)$$

where τ_{rel} denotes the relaxation time in Landau–Lifshitz form. They are complex where the imaginary parts of μ and κ are associated with the ferrite losses. However, in this section we shall consider the case of lossless ferrite ($\tau_{rel} = \infty$) so that we may more strongly illustrate the resonance phenomena. The results for the case of the thin rod inserted at the center of the waveguide ($x_0 = a/2$) are considered here (see Fig. 1). For the numerical values of parameters, we chose the case that the saturation magnetization $4\pi M_s = 1200$ G, the dielectric constant $\epsilon_r = 14.0$, the radius of rod $\rho = 1.0$ mm, the frequency $\omega/2\pi = 4.0$ GHz, and the width of the rectangular waveguide $a = 58.1$ mm.

The infinite series h_{np} represented by [3, eq. (33)] is extremely slowly convergent and is not suitable for the numerical computation. Therefore, we transformed it to the rapidly convergent series by using Euler's transformation of series [5] and obtained its value. Then we solve the equations with $p = 0, \pm 1, \pm 2, \pm 3$, and ± 4 in [3, eq. (33)] (truncation size equals 4). Also, in the case of truncation size 15, the same numerical solution was obtained; therefore, it seems that the coefficients A_p and B_p were determined with adequate accuracy.

A. Transmission and Reflection Coefficients

In Fig. 2, the amplitudes of the computed transmission and reflection coefficients are shown as a function of internal static magnetic field. The transmission and reflection coefficients have minima and maxima, respectively, in 964, 955, 952, 951, $\cdots$ Oe and 842 Oe. In fields far lower than 842 Oe and far higher than 964 Oe, the amplitude of the reflection coefficient is approximately constant ($\simeq 0.1$), which implies that in these regions the ferrite rod acts as a dielectric material rather than as a ferrimagnetic one. Moreover, the amplitude

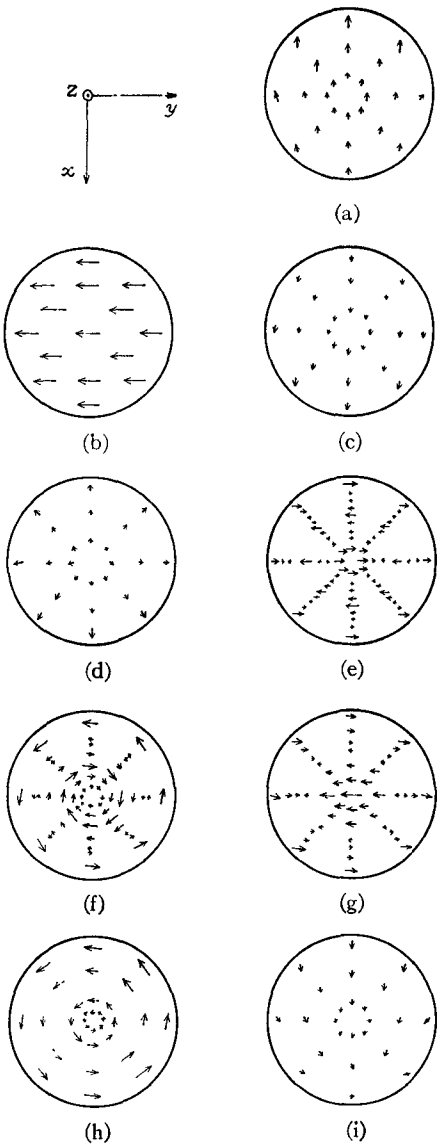

Fig. 3. RF magnetization distribution on the xy cross section of the ferrite rod (at time $t=0$). (a) 600 Oe. (b) 842 Oe (resonance). (c) 871 Oe. (d) 947 Oe. (e) 951 Oe (resonance). (f) 952 Oe (resonance). (g) 955 Oe (resonance). (h) 964 Oe (resonance). (i) 1200 Oe.

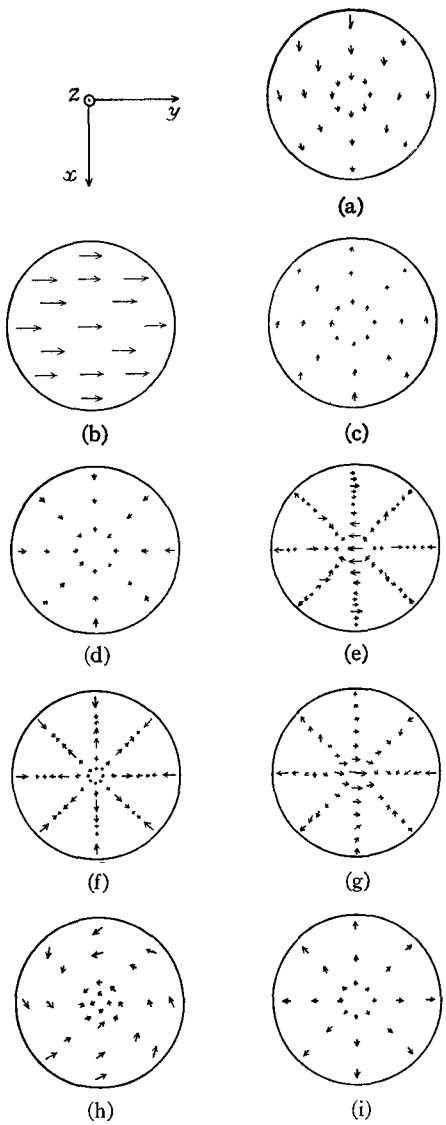

Fig. 4. RF magnetic field distribution on the xy cross section of the ferrite rod (at time $t=0$). y is the propagation direction. (a) 600 Oe. (b) 842 Oe (resonance). (c) 871 Oe. (d) 947 Oe. (e) 951 Oe (resonance). (f) 952 Oe (resonance). (g) 955 Oe (resonance). (h) 964 Oe (resonance). (i) 1200 Oe.

of the reflection coefficient for fields between 871 and 947 Oe is small compared with the value in the case of a dielectric material. Particularly in 871 and 947 Oe, the reflection coefficient becomes almost completely zero.

In the lossless case, the transmission coefficient S_{21} and the reflection coefficient S_{11} must satisfy the following relation [6]:

$$|S_{11}|^2 + |S_{21}|^2 = 1 \tag{4}$$

which is the energy conservation law. In practice, our computed results satisfy (4) with the accuracy of $10^{-6} \sim 10^{-8}$ at all static magnetic field values. This means that our computation is performed with adequate accuracy. The results of Okamoto *et al.* satisfied (4) only within the accuracy of $10^{-1} \sim 10^{-2}$ (our computation is performed in the case $k_0\rho = 0.0837$).

B. Magnetization and Magnetic Field Distributions

We can obtain the RF magnetization and magnetic field from [3, eq. (8)] and Maxwell's equations. Fig. 3 shows the RF magnetization distribution (at time $t=0$) inside the rod. At field values where the amplitude of transmission (reflection) coefficient is a minimum (maximum), the computed magnetization amplitude becomes very large compared with the amplitude in other fields, suggesting that resonance occurs. The magnetization distribution for the resonance in 842 Oe is uniform and the distributions for the resonances in 964, 955, 952, and 951 Oe, etc., have good symmetrical patterns. The magnetization at an arbitrary point in the rod is circularly polarized counterclockwise with a period of $2\pi/\omega$. The RF magnetic field distribution inside the rod is shown in Fig. 4. At resonance, it has a good symmetri-

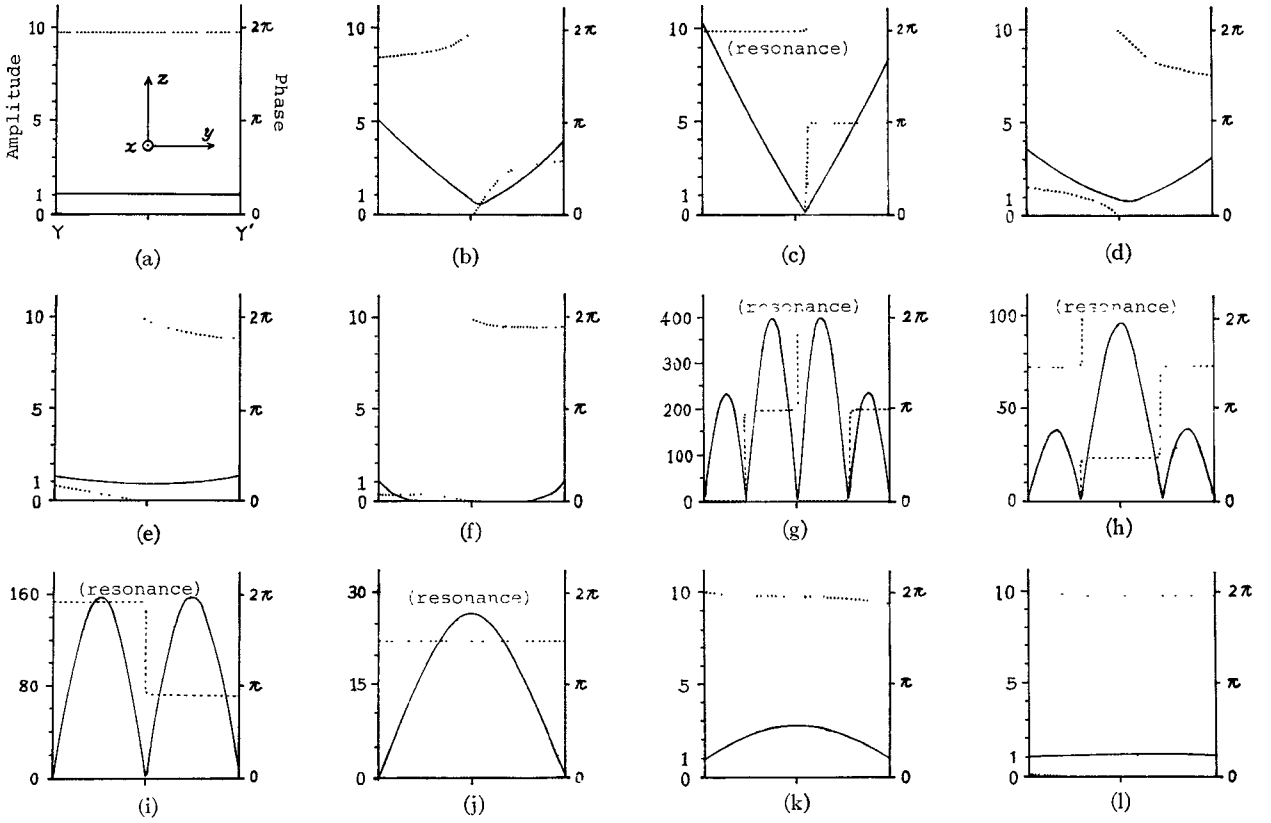

Fig. 5. Electric field (E_z') distribution on the diameter YY' of the cross section of the ferrite rod (at time $t=0$). [Amplitude (solid line); phase (dotted line).] (a) 600 Oe. (b) 838 Oe. (c) 842 Oe. (d) 848 Oe. (e) 871 Oe. (f) 947 Oe. (g) 951 Oe. (h) 952 Oe. (i) 955 Oe. (j) 964 Oe. (k) 978 Oe. (l) 1200 Oe.

cal pattern as well as the magnetization distribution. The magnetic field distribution can be understood by considering the magnetization in Fig. 3.

C. Electric Field Distribution

The electric field distribution (at time $t=0$) on the diameter $YY'(x=a/2)$ of the xy cross section is illustrated in Fig. 5 (y is the propagation direction). The amplitude of electric field E_z' at resonance is very large compared with the amplitude of the incident electric field $E_0(=1)$.

In view of the physical meaning for resonances, we review [3, eq. (8)], which represents the electric field inside the rod. In Fig. 6, the values of k and $k\rho$ are shown as a function of static magnetic field. The values of k and $k\rho$ at the representative resonances and the nearest zeros j_{mn} ($n=1, 2, \cdots$) of the Bessel function to these values of $k\rho$ are tabulated in Table I.

At the resonances in 964, 955, 952, and 951 Oe, etc. (values of k are real), the electric field is trapped in the rod and forms the standing wave with large amplitude. This resonance is one of the standing wave modes (volume modes). This may be seen from the fact that we can find the zero of the Bessel function, which approximately agrees with the value of $k\rho$. In Fig. 5(g)–(j), the electric field amplitude is a maximum where the direction of magnetization is reversed in Fig. 3.

On the other hand, at the resonance in 842 Oe the electric field is trapped on the rod surface and its amplitude decreases toward the center of the rod (a surface mode). This may be understood by considering that the value of k is imaginary. The RF magnetization distribution for this resonance is uniform, as described in Sec-

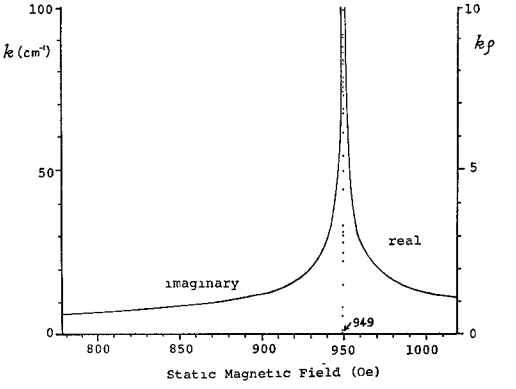

Fig. 6. k and $k\rho$ ($\rho=0.1$) as a function of static magnetic field intensity.

TABLE I

$k\rho$ AND THE NEAREST ZERO TO $k\rho$

Static magnetic field (Oe)	$k\rho$	The nearest zero to $k\rho$
842	0.81 j	
950	8.62	j_{03} = 8.65
951	6.96	j_{13} = 7.02
952	5.49	j_{02} = 5.52
955	3.75	j_{11} = 3.83
964	2.33	j_{01} = 2.40

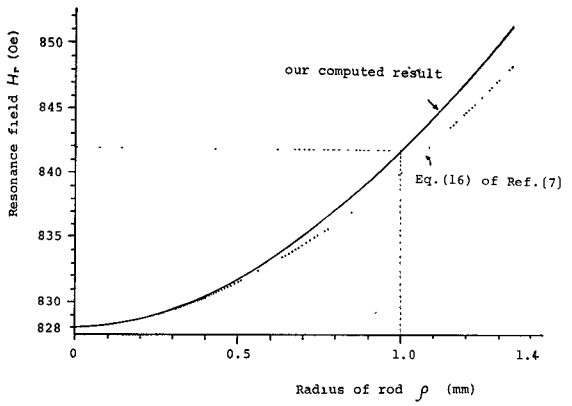

Fig. 7. Resonance field as a function of the radius of the rod.

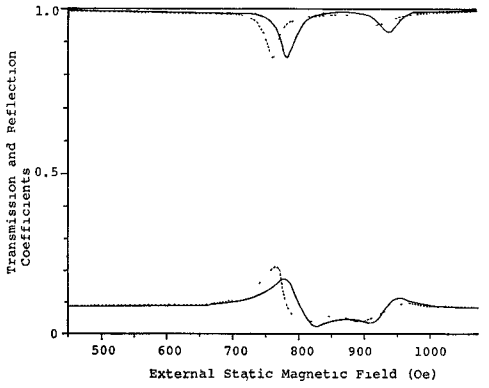

Fig. 8. Amplitudes of transmission and reflection coefficients as a function of external static magnetic field intensity. Theoretical value (solid line); experimental value (dotted line).

tion II-B, and this resonance is one of the magnetostatic modes.

Disregarding the size effect [7] ($k_0\rho \to 0$), the resonance field H_{r0} of the magnetostatic mode for the infinite long circular cylindrical rod is given by the following relation [8] (γ the gyromagnetic ratio):

$$H_{r0} = \frac{\omega}{\gamma} - 2\pi M_s = 828 \text{ Oe}. \tag{5}$$

Also, this relation can be easily obtained from the magnetostatic equation (rod $\boldsymbol{H}=0$). Fig. 7 shows the resonance field H_r computed in our analysis and given [7, eq. (16)] when the radius of the rod is changed. When $\rho \to 0$, the computed resonance field approaches H_{r0}. The shift from H_{r0} of the resonance field may be explained by the size effect.

In Fig. 5(b)–(d), there exists a reduction in the electric field on the shadow side (Y') of the rod. This seems to be a "shadow" effect because the reduction decreases in a thinner rod.

III. Experimental Results

We measured the amplitudes of the transmission and reflection coefficients for a lossy ferrite rod. The experiments were performed at 4.0 GHz for a polycrystalline ferrite rod: $\rho = 1.0$ mm, $4\pi M_s = 1340$ G, and $\epsilon_r = 14.0$.

In Fig. 8, the experimental results are shown for the case in which the rod is located at the center of the waveguide. Also in Fig. 8, the theoretical values in which $\tau_{rel} = 4.0 \times 10^{-9}$ s (losses were included in the analysis) are shown for comparison with the experimental results. In this figure, many peaks in Fig. 2 disappear by relaxation processes, and then only two representative peaks remain.

The experimental results agree well with the theoretical values. The slight difference in them may be due to the fact that the theoretical values are obtained by neglecting the anisotropy magnetic field in the ferrite.

IV. Conclusion

For the axially magnetized circular cylindrical ferrite rod inserted parallel to the E-field of the TE_{10} mode in the rectangular waveguide, the transmission and reflection coefficients and the electromagnetic field inside the rod were numerically computed and their results are shown in figures. We illustrated two types of resonance phenomena: the magnetostatic mode and the standing wave mode.

The experimental results of transmission and reflection coefficients agree well with the theoretical values.

We think this kind of study might be a great help in attacking the problems of the excitation of spin wave and its propagation in ferrite, and also of the interactions of electromagnetic waves between ferrites and semiconductors [9], [10] and of the nonreciprocal devices.

Acknowledgment

The authors wish to thank K. Kozuka and K. Kawasaki for their fruitful discussions.

References

[1] K. Kozuka, M. Umeno, T. Yoshida, and S. Miki, "Modes of resonance absorptions of magnetostatic waves in axially magnetized YIG rods," *Jap. J. Appl. Phys.*, vol. 11, pp. 190–196, Feb. 1972.

[2] P. S. Epstein and A. D. Berk, "Ferrite post in rectangular wave guide," *J. Appl. Phys.*, vol. 27, pp. 1328–1335, Nov. 1956.

[3] N. Okamoto, I. Nishioka, and Y. Nakanishi, "Scattering by a ferrimagnetic circular cylinder in a rectangular waveguide," *IEEE Trans. Microwave Theory Tech.*, vol. MTT-19, pp. 521–527, June 1971.

[4] T. Yoshida, M. Umeno, and S. Miki, "Propagation characteristics in the waveguide loaded with a cylindrical rod of magnetized ferrite," presented at the Int. Symp. Antennas and Propagation, Sept. 1971, Paper 1-IIIC4.

[5] *Handbook of Mathematical Functions with Formulas, Graphs, and Mathematical Tables* (Applied Mathematical Series 55). Washington, D. C.: NBS, 1964, p. 16.

[6] R. E. Collin, *Foundations for Microwave Engineering*. New York: McGraw-Hill, 1966, p. 177.

[7] R. Plumier, "Size effect for magnetostatic mode of the type (n, n, o) in a ferrite cylinder," *Physica*, vol. 27, pp. 403–405, 1961.

[8] B. Lax and K. J. Button, *Microwave Ferrites and Ferrimagnetics*. New York: McGraw-Hill, 1962, p. 164.

[9] K. Kozuka, M. Umeno, Y. Kamo, and S. Miki, "A new type microwave element composed of YIG and semiconductor crystals," in *Proc. 2nd Conf. Solid State Devices*, vol. 40, pp. 244–250, 1971.

[10] M. Umeno, K. Kawasaki, K. Kozuka, and S. Miki, "Interaction of spin wave in YIG single crystals with carriers in semiconductors," presented at the Int. Conf. Ferrite (Kyoto, Japan, July 1970), Paper 9A 3.5.